International Journal of Automation and Control

ISSN online: 1740-7524 - ISSN print: 1740-7516
https://www.inderscience.com/ijaac

Development of modified LQG controller for mitigation of seismic vibrations using swarm intelligence

Gaurav Kumar, Roshan Kumar, Ashok Kumar, Brij Mohan Singh

DOI: 10.1504/IJAAC.2023.10049079

Article History:

Received:	20 March 2021
Last revised:	20 July 2021
Accepted:	05 August 2021
Published online:	30 November 2022

Development of modified LQG controller for mitigation of seismic vibrations using swarm intelligence

Gaurav Kumar*

Department of Electronics and Communication Engineering,
ACED,
Alliance University,
Bengaluru, Karnataka 562106, India
Email: gaurav.kumar@alliance.edu.in
*Corresponding author

Roshan Kumar

School of Electronic and Information Technology,
Miami College of Henan University,
Henan, China
Email: roshan.iit123@henu.edu.cn

Ashok Kumar

Department of Earthquake Engineering,
Indian Institute of Technology,
Roorkee, Uttarakhand, India
Email: akmeqfeq@iitr.ernet.in

Brij Mohan Singh

Department of Computer Science and Engineering,
College of Engineering Roorkee,
Uttarakhand, India
Email: brijmohansingh@coer.ac.in

Abstract: A method is presented to design and tune the modified linear quadratic Gaussian (LQG) controller to obtain increased efficiency during an earthquake. It utilises swarm intelligence to tune the parameters of LQG based on quasi resonance between the natural frequencies of the structure in first two modes and the predominant frequencies of the seismic signal. The modified controller thus developed minimises the energy of structure by altering its parameters online. For testing of this modified controller, a benchmark prototype structure is numerically tested under different seismic signatures recorded in near/far fault sites in the different soil conditions. A parametric study comparing the efficiencies of modified LQG, and other contemporary controllers is presented. It is observed for El-Centro earthquake that the modified controller achieved reductions of 22%, 33% and 27% in relative displacement, inter-storey drift, and absolute acceleration respectively

as compared to the conventional LQG controller. Similar results are observed for Gebze and Chi-Chi earthquakes. The modified controller is also evaluated in a situation where power vanishes at the peak of the seismic excitation. Based on the results and discussion, the performance of the proposed controller is observed to be superior among all controllers considered in this study.

Keywords: semi-active control; magneto-rheological damper; seismic vibrations; optimal control; particle swarm optimisation; linear quadratic Gaussian; LQG.

Reference to this paper should be made as follows: Kumar, G., Kumar, R., Kumar, A. and Singh, B.M. (2023) 'Development of modified LQG controller for mitigation of seismic vibrations using swarm intelligence', *Int. J. Automation and Control*, Vol. 17, No. 1, pp.19–42.

Biographical notes: Gaurav Kumar received his PhD in Optimal Controller Design from the Indian Institute of Technology (IIT) Roorkee, Uttarakhand, India. He is an Associate Professor at the SENSE, VIT University, Vellore, Tamil Nadu India. His research domain includes optimal controller design, seismic signal processing and swarm intelligence.

Roshan Kumar received his PhD in Signal Processing and Structural health monitoring from the Indian Institute of Technology (IIT) Roorkee, Uttarakhand, India. He is an Assistant Professor at the Department of Electronic and Information Technology, Miami College of Henan University, Henan China. His research domain is seismic signal processing and Structural Health Monitoring.

Ashok Kumar received his PhD in Mechanical Engineering from the IIT Roorkee, Uttarakhand, India. He retired as a Professor from the Department of Earthquake Engineering, IIT Roorkee. His research domain is related to strong motion analysis, seismic instrumentation, earthquake early warning system.

Brij Mohan Singh received his PhD in Computer Science and Engineering from the UTU, Dehradun, Uttarakhand, India. He is a Professor at the Department of Computer Science and Engineering, College of Engineering Roorkee. His research interests are pattern recognition and image processing.

1 Introduction

The seismic vibrations can cause the failure of the infrastructures resulting in huge monetary losses and loss of human lives. Generally, the inherent low damping of the structure makes these structures prone to the damage amid a seismic occurrence. Therefore, during the earthquake, altering stiffness and damping of the structure using control schemes could be a very useful measure for mitigating the seismic vibrations (Housner et al., 1997). However, the structural control is well documented in the literature (Symans and Constantinou, 1999; Amezquita-Sanchez et al., 2014; Saaed

et al., 2015; Kandasamy et al., 2016), Table 1 summarises the control schemes based on their characteristics and devices used. Referring to Table 1, the performance of semi active control (SCS) matches to that of active control (ACS) without requiring high electric power to operate. Moreover, it maintains structural integrity by absorbing the seismic energy from the structure without adding any extra energy. Thus, the bounded input and bounded output (BIBO) property inherently exists in the SCS (Garrido et al., 2018).

Table 1 Characteristics of the structural control schemes and example devices

S. no.	*Classification*	*Characteristics*	*Example devices*
1	Passive control	Requires no additional energy	Tuned mass damper (TMD), tuned liquid column damper (TLCD), visco-elastic damper (VED)
2	Active control	Need high power to generate the restoring force	Active mass damper (AMD), active tendons
3	Semi-active control	• It requires very less power to operate • It can produce only dissipative forces	Semi-active TMD, magneto-rheological dampers (MRDs), electro-rheological dampers (ERDs)

Figure 1 demonstrates the block diagram of SCS which consists of a structure-actuator assembly (MR damper in the present study) and the controller. It is observed that the efficiency of SCS depends on the controller (Bhaiya et al., 2019; Fessi and Bouallègue, 2019). The fellow researchers explored the possibilities for incorporating modern control theory in the field of vibrations control to make the SCS more effective. Moreover, the phenomenal growth of the signal processing techniques and the advent of highly efficient digital signal processors facilitate the deployment of complete control system on a single silicon chip. These fast-computing devices not only helped to reduce the chance of possible damage to the installations in the seismic environment but also enable engineers to design real-time systems. Impediments during the development of a controller depend on the modelling of structure, uncertain and noisy environment, stability, feedback planning (centralised/decentralised) and the nonlinearity present in the structure (Kumar et al., 2018).

The controller viz. sliding mode (SMC), quasi bang-bang (QBB), linear quadratic regulator (LQR), simple passive control (SPC), neural network, fuzzy controller, etc. are discussed in literature (Jansen and Dyke, 2002; Collins and Selekwa, 2002; Choi et al., 2004; Dong et al., 2010; Choi et al., 2016; El-Sayed et al., 2021; Boulaaras, 2017; Boulaaras and Doudi, 2020). As observed, these controllers are successful for a specific class of structures but may be inadequate for another class (Casciati et al., 2012). This unpredictable performance of the controller is obtained due the assumptions made by the developers while design the controller (Chandrasekar et al., 2021). Therefore, prior knowledge of the structure and its mathematical model, nature of uncertainties, elements of the used actuators are necessary to design an optimal controller (Spencer and Nagarajaiah, 2003).

Figure 1 Semi-active control scheme

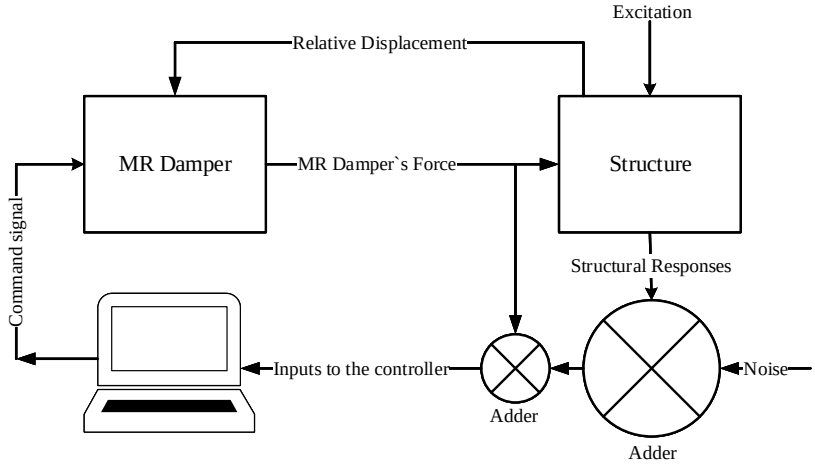

In optimal control theory, there is a cost function which has to be minimised to achieve the optimal results. This cost used to be a function of variable(s) of the system under consideration. A popular optimal controller (viz. LQR) based on the linear quadratic theory, has been used extensively in structural control (Symans and Constantinou, 1999; Wu, 2017; Sari et al., 2020; Miladi et al., 2021; Abdalla et al., 2021). This controller in conjunction with the on-off switch-based control mechanism (viz. clipped control law) determines a command signal to the MRD. The damper's force is used as a feedback to generate an appropriate command signal (Dyke et al., 1996a, 1996b). The performances of the popular controllers viz. decentralised bang-bang controller, moderated homogeneous friction procedure and the Lyapunov stability criteria-based controller to the clipped optimal (CO) LQR has been carried out by Jansen and Dyke (2002). It is observed that the LQR control algorithm does not consider the measurement/sensor noise and the process noise even though these remain present all the time. For theoretical purposes, researchers modelled this noise as the Gaussian white noise. A filter known as Kalman observer is used to estimate the future states of the system adequately in presence of the noise in LQG controller (Dyke et al., 1996a; Askari et al., 2011; Barkefors et al., 2014).

In LQG controller, the selection of appropriate weighting matrices for minimisation of the cost function is difficult. These are determined by the trial-and-error method. These matrices [equation (3)] have global values and these matrices cannot be altered with the varying circumstances during the earthquake. The alteration in these matrices is a necessity because the counter-force requirement from the damper may change during its operation. The control weighting matrix (CWM) **R** in LQG controller is directly related to the counter-force determination. Thus, the fellow researchers investigated effective methods to update these matrices when required during the earthquake (Miyamoto et al., 2018; Shafieezadeh et al., 2008). An algorithm based on a repository of the earthquakes was presented by Panariello et al. (1997). The authors uprooted the necessity of trial-and-error to ascertain suitable gain matrices. However, the online alteration of weighting matrices was not possible since these were chosen on the basis of repository. The properties of discrete wavelet transform (DWT) were utilised to develop a time variable LQR (TVLQR) method by Basu and Nagarajaiah (2008). The

CWM (**R**) was updated online by multiplying with a constant. The multiplier was determined on the basis of energy content in different sub-intervals of the structural response to regulate the control force. An offline repository of known earthquakes same as presented in Panariello et al. (1997) was used to choose the constant multiplier of **R** (Basu and Nagarajaiah, 2008, 2010). Further, a modified LQR tuned with genetic algorithm (GA) was proposed to alter **R**, where the GA was employed to determine the weighting matrices (Wongsathan and Sirima, 2008). The use of GA optimisation enabled the alteration of **R** almost online. The slow convergence in the GA was a limitation in this method.

For seismic environment, developing a fast, optimal, realisable and robust controller is necessary to dispense an appropriate command signal to the MRD. Present work aims at the development of modified LQG control algorithm for SCS to attain better performance in reducing the structural responses. The quasi resonance between the earthquake and the natural frequency of structure is computed using a fast Fourier transform (FFT). It is known that the magnitude of the vibrations become large at resonance consequently, a high counter-force will be needed and vice-versa. The LQG controller is modified to dispense a more appropriate control-force in the resonance conditions. The proposed controller is validated on a three-storey structure under El-Centro, Gebze and Chi-Chi earthquake time histories by comparing its results to the conventional LQG controller and other popular controllers presented in Dyke et al. (1996b).

2 Theory

2.1 Linear quadratic Gaussian controller

In the implementation of the LQR controller, availability of all states is assumed at every instant. Practically, this is difficult in case of earthquake as sudden changes in structural responses may occur. The controller may not function properly without knowing the correct states. In these circumstances, a more intelligent controller like LQG is required which is capable of observing the next state if it is not available. The LQG controller is the combination of the LQR controller and the Kalman filter.

Further, a structure is assumed as a linear time-invariant (LTI) system represented in state space domain by equations (1)–(2).

$$\dot{z_t} = \mathbf{A}z_t + \mathbf{B}u + \mathbf{E}w \tag{1}$$

$$y_t = \mathbf{C}z_t + \mathbf{D}u + v \tag{2}$$

where u is force, z_t is state vector, y_t is measured output. For n-DOF system, these matrices $\mathbf{A}, \mathbf{B}, \mathbf{C}, \mathbf{D}$ and $\mathbf{E}$ are given by equations (17)–(21). w and v are the disturbance input and measurement error respectively. Both are assumed as uncorrelated and white Gaussian random process with zero means. For this system, an infinite horizon global cost function is defined as given in equation (3).

$$J(z_t, u) = \int_0^\infty (z_t^T Q z_t + u^T R u) dt \tag{3}$$

The **Q** is the state weighting matrix (SWM) and it is semi definite whereas **R** is the control weighting matrix (CWM) and it is a positive definite matrix. The LQG controller that solves the LQG control problem is formulated as in equations (4) and (5).

$$\dot{\hat{z}}_t = \mathbf{A}\hat{z}_t + \mathbf{B}u + \mathbf{L_{Kal}}(y_t - \mathbf{C}\hat{z}_t - \mathbf{D}u) \tag{4}$$

$$u = -\mathbf{K_{LQR}}\hat{z}_t \tag{5}$$

Here, $\hat{z}$ is the observed state or the next estimated state. The calculation of the Kalman filter gain $\mathbf{L_{Kal}}$ and the LQR controller gain $\mathbf{K_{LQR}}$ are carried out separately using the algebraic Riccati equation (ARE) by calculating covariance estimate matrix ($\mathbf{P_{Kal}}$). These gains are given independently by equations (6) and (7) assuming **V** is the spectral density matrix related to the measurement noise v.

$$\mathbf{L_{Kal}} = \mathbf{R}^{-1}\mathbf{B}^{\mathbf{T}}\mathbf{P_{LQR}} \tag{6}$$

$$\mathbf{K_{LQR}} = \mathbf{V}^{-1}\mathbf{C}^{\mathbf{T}}\mathbf{P_{Kal}} \tag{7}$$

The Kalman filter is used as an observer by measuring the available data. This observer minimises the spread of the estimate error probability density in the process. The block diagram for the LQG controller is shown in Figure 2.

Figure 2 LQG controller (see online version for colours)

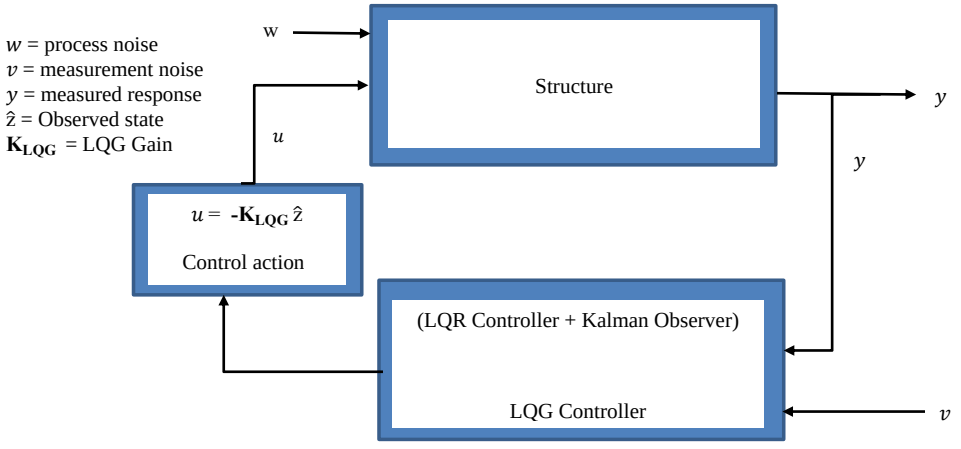

2.2 Particle swarm optimisation

Particle swarm optimisation (PSO) is a heuristic approach and, it was proposed by Kennedy and Eberhart in 1995. This approach resembles the social behaviour of the birds to find a new route. There is a group of individuals called the population. Each individual (i.e., particle) is equivalent to a bird in its group (i.e., population). Particle alters its position and velocity regularly to identify the best possible value (i.e., particle best) in the exact same way as the bird alters its path in a group. Further, there is a global best of the entire population which decides the final value of alteration at any given instant. The particle best as well as the global best are calculated by

minimisation of a cost function. So, it can be said that the PSO is a collaborative optimisation technique. However, several variants of PSO have been developed by the fellow researchers which have very good convergence speed, stable solution for different cost functions and do not trap in local optima. The classical PSO is sufficient for present work as the number of variables is less and it is easily implementable. The details on the PSO algorithm may be studied in Amini and Samani (2014), Ullmann et al. (2017), Maiti et al. (2018), Abderrezek et al. (2019) and Hu et al. (2020). Table 2 represents the parameters employed here.

Table 2 Parameters used for implementation of PSO

Parameter	*Value*
Inertia weighting factor δ	0.6
Acceleration constants c_1 and c_2	2
Random sample b_1 and b_2	0.3
Loops	50
Population size	50

The cost function (J_{PSO}) minimised in this work is a function of inter-storey drift between n^{th} and $(n-1)^{\text{th}}$ and mathematically represented as in equation (8)

$$J_{PSO} = \int_0^t [z_n - z_{n-1}]dt \tag{8}$$

We know that, the inter-storey drift is defined as the difference between two subsequent floors. In equation (8), the z_n and z_{n-1} are the displacement of n^{th} and $(n-1)^{\text{th}}$ floors of the structure respectively.

2.3 Development of modified LQG controller

It is evident that the structural responses have similar properties as earthquake time histories. These are non-stationary signal having numerous frequency components. It is possible that frequency components of the earthquake signal and the natural frequencies of the structure may coincide or come in the proximity. This can cause a quasi-resonance where the magnitude of structural responses will be the largest. In such circumstances, a higher control force is needed for effective mitigation seismic vibrations. To get optimal results from conventional LQG controller a quadratic cost function [see equation (3)] is minimised by varying the SWM '**Q**' and CWM '**R**'. These matrices are determined while designing the controller through trial-and-error method. There is no mechanism to update these matrices during operation to deliver apt control force. It is a serious drawback that needs to be resolved appropriately.

Figure 3 Development of modified LQG controller using PSO-FFT approach (see online version for colours)

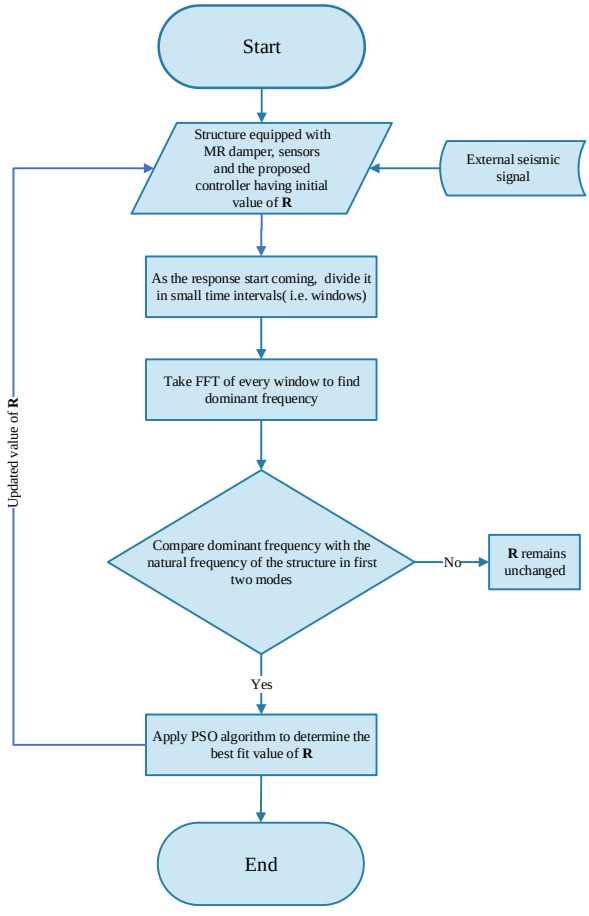

For solution, the structural response having total time length from 0 to t is divided into smaller sub-time intervals. These intervals are known as window having length 1 sec. The frequency having maximum amplitude (i.e., dominant frequency) for each window is calculated using the fast Fourier transform (FFT). Now, the PSO algorithm is used to tune up the value of CWM in the selected range at these quasi resonances which provides the optimal value of CWM for optimum structural response with lesser control effort. The PSO algorithm has computational cost but, the phenomenal growth of digital signal processors made it possible to do the calculation in real time and a negligible time delay will not affect the methodology. Using PSO for sub time intervals can be thought as if the CWM has a local solution instead of a global solution. The advantage of this local solution is that it can alter the CWM as per the requirement. For modified LQG, the cost function is formulated for any w_{th} window and, it is given by equation (9).

$$J_w(z,u) = \int_0^t (\mathbf{z}^T \mathbf{Q_w} \mathbf{z} + \mathbf{u}^T \mathbf{R_w} \mathbf{u}) dt \tag{9}$$

where **z** is the displacement of the structure, **u** is the control force, $\mathbf{Q_w}$ is the SWM and $\mathbf{R_w}$ is the CWM for the w^{th} window respectively. A control law presented by equation (10) is the solution of cost function $J_w(z,u)$ for any window.

$$u = -[\mathbf{G_w}]z \tag{10}$$

The gain matrix $\mathbf{G}_w$ can be obtained by solving the Ricatti differential equation all small time windows which initiates the command signal for the MRD. The distinction of the PSO-FFT-based modified LQG controller is that CWM is computed online as per requirement of the system by PSO algorithm contrary to the method discussed in Basu and Nagarajaiah (2008).

3 Case study

3.1 Modelling of the three-storey structure

A prototype structure (see in Figure 4) is employed here for validation of the proposed controller. It is widely used scaled model of the benchmark three-storey structure having scaling factors same as reported in Dyke et al. (1996b) and Choi et al. (2004). The first two fundamental frequencies are compared with the dominant frequency of each interval (i.e., 1 sec). The displacement of each floor is x_1, x_2 and x_3 respectively whereas the accelerations of the respective floors are denoted as $xa1, xa2$ and $xa3$ as shown in Figure 4.

Figure 4 Test structure comprised of accelerometers and MR damper (see online version for colours)

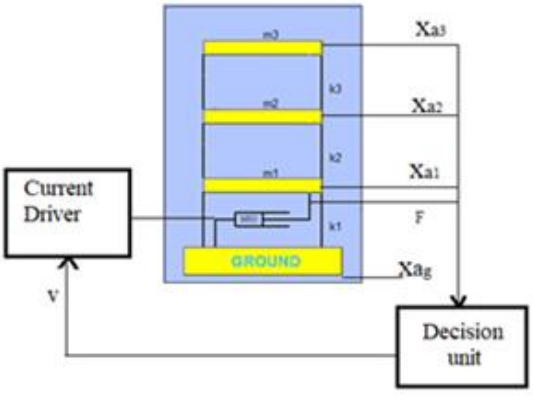

Considering the overall system (structure and MRD) linear and time-invariant for simplicity, the dynamic behaviour of the system can be expressed mathematically in equation (11).

$$\mathbf{M_t}\ddot{z}_t + \mathbf{C_t}\dot{z}_t + \mathbf{K_t}z_t = \Gamma u + \mathbf{M}\Lambda\ddot{x}_{a_g} \tag{11}$$

where $\mathbf{M_t}$ is a mass matrix, $\mathbf{C_t}$ is damping matrix, $\mathbf{K_t}$ is the stiffness matrix. The parameters shown in equations (12)–(14) are alike as presented in Dyke et al. (1996b).

The relative displacement response vector $\mathbf{z}$ due to the unidirectional excitation $\ddot{x}_{a_g}$ has a dimension (3×1). The variable u specifies the control force and Λ specifies a column vector of ones. The column vector Γ ascertain the MRD's position in the structure. The MRD's displacement z_{MR} is assumed equivalent to the displacement of the first floor z.

$$\mathbf{M_t} = \begin{bmatrix} 98.3 & 0 & 0 \\ 0 & 98.3 & 0 \\ 0 & 0 & 98.3 \end{bmatrix} \tag{12}$$

$$\mathbf{C_t} = \begin{bmatrix} 175 & -50 & 0 \\ -50 & 100 & -50 \\ 0 & -50 & 50 \end{bmatrix} \tag{13}$$

$$\mathbf{K_t} = \begin{bmatrix} 1{,}200{,}000 & 684{,}000 & 0 \\ -684{,}000 & 1{,}370{,}000 & -684{,}000 \\ 0 & -684{,}000 & 684{,}000 \end{bmatrix} \tag{14}$$

Another representation of mathematical equation (EOM) of the system in time domain is exhibited through equations (15)–(16).

$$\mathbf{z_t} = \mathbf{A}z_t + \mathbf{B}u + \mathbf{E}x_{a_g} \tag{15}$$

$$\mathbf{y} = \mathbf{C}z_t + \mathbf{D}u \tag{16}$$

where u is force produced by the MRD, z_t is state vector, $\mathbf{y}$ is measured output. For n-DOF system, these matrices $\mathbf{A}, \mathbf{B}, \mathbf{C}, \mathbf{D}$ and $\mathbf{E}$ are given as in equations (17)–(21).

$$\mathbf{A} = \begin{bmatrix} \mathbf{0_{n\times n}} & \mathbf{I_{n\times n}} \\ -\mathbf{M_{t_{n\times n}}^{-1}}\mathbf{K_t} & -\mathbf{M_{t_{n\times n}}^{-1}}\mathbf{C_t} \end{bmatrix} \tag{17}$$

$$\mathbf{B} = \begin{bmatrix} \mathbf{0_{1\times n}} \\ -\mathbf{M_{t_{n\times n}}^{-1}}\Gamma \end{bmatrix} \tag{18}$$

$$\mathbf{E} = \begin{bmatrix} \mathbf{0_{1\times n}} \\ \Lambda \end{bmatrix} \tag{19}$$

$$\mathbf{C} = \begin{bmatrix} -\mathbf{M_{t_{n\times n}}^{-1}}\mathbf{K_t} & -\mathbf{M_{t_{n\times n}}^{-1}}\mathbf{C_t} \\ \mathbf{I_{n\times n}} & \mathbf{0_{n\times n}} \\ \mathbf{0_{n\times n}} & \mathbf{I_{n\times n}} \end{bmatrix} \tag{20}$$

$$\mathbf{D} = \begin{bmatrix} -\mathbf{M_{t_{n\times n}}^{-1}}\Gamma \\ \mathbf{0_{1\times n}} \end{bmatrix} \tag{21}$$

The accelerations of all floors and MRD displacement measurements are essential to calculate suitable control action. These structural measurements are easily obtainable using appropriate sensors in the laboratory.

3.2 Modelling of the MR damper

The MRDs of different sizes and capacities are available in the market. The appropriate MRD is determined according to the structure.

Figure 5 MR Damper, (a) hardware structure (b) working principle (see online version for colours)

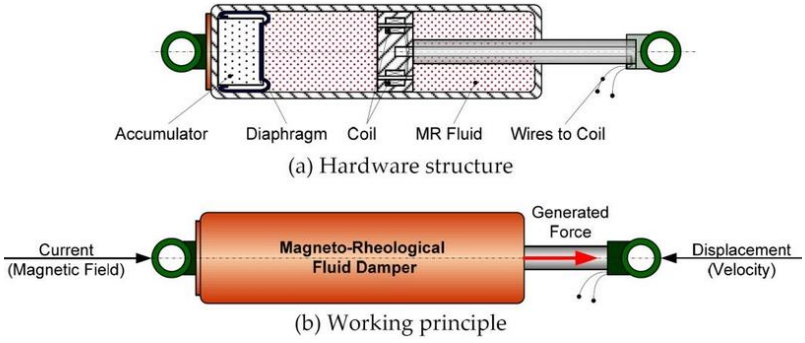

Figures 5(a)–5(b) show the hardware and the working principle of MRDs considered in this numerical study. A nominal magnetic field is generated by a tiny electromagnet which is enough for the operation of MRD. It is also reported in literature that a force up to 200 kN can be generated very quickly (in 60 ms) with a very small power (50 W) (Yang et al., 2004). Different models such as Bouc-Wen, Bingham, polynomial, and tangent hyperbolic model have been discussed in Spencer et al. (1997) and Ismail et al. (2009).

A comprehensive diversity of hysteric behaviour is shown in simple Bouc-Wen model in Figure 6(a). This model provides the force-displacement behaviour and retains force-velocity characteristics of the MRD like the experimentally obtained results presented in Spencer et al. (1997). The force-velocity characteristics of the MRD is nonlinear and there is no roll-off at low velocities where force and velocity have opposite signs.

Figure 6 (a) Simple Bouc-Wen model (b) Modified Bouc-Wen model

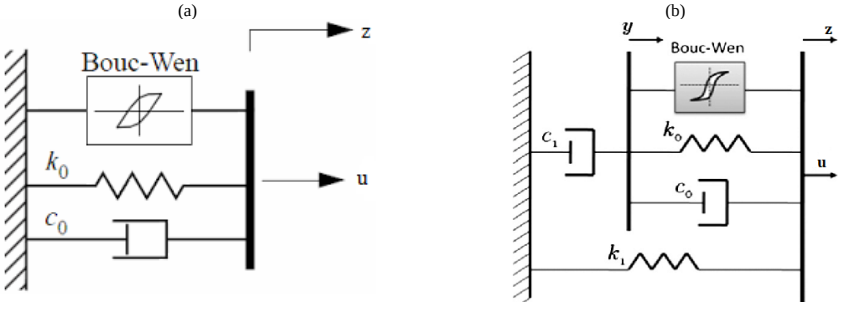

To conjecture the damper's response at small velocities as shown in Figure 6(b) a modified Bouc-Wen model was presented in Spencer et al. (1997). The upper section of this model drives the dynamic equations of the MRD. The forces on any side of the rigid bar are comparable. The MR damper force is a function of the velocity and displacement of the MRD. Equations (22)–(28) are used to simulate this model. During the simulation, damper produces a force u is directly linked to the voltage enforced to

the damper and is defined in equation (22). From equations (25)–(29), it can be inferred that these variables quantities are proportional to the effective voltage u_0.

$$u = c_1 y + k_1(z_x - z_0) \tag{22}$$

$$\dot{z_1} = -\gamma|\dot{z_x}| - \dot{z_y} z_1 |z_1|^{n-1} - \beta(\dot{z_x} - \dot{z_y})|z_1|^n + A(\dot{z_x} - \dot{z_y})|z_1 \tag{23}$$

$$z_y = \frac{1}{c_0 + c_1}\alpha z_1 + c_0 \dot{z_x} + k_0(z_x - z_y) \tag{24}$$

$$\alpha = \alpha_a + \alpha_b u_0 \tag{25}$$

$$c_0 = c_{0a} + c_{0b} u_0 \tag{26}$$

$$c_1 = c_{1a} + c_{1b} u_0 \tag{27}$$

$$\dot{u_0} = -\eta(u_0 - v) \tag{28}$$

Here, k_1 is accumulator's stiffness, k_0 is stiffness at large velocities, z_0 is displacement of spring due to k_1, c_0 and c_1 are low velocities, z_1 is an evolutionary variable, γ, β, n and A are used to take care of nonlinearity of the MR damper called as the controllable parameters. Equation (28) is used to drive the electromagnet in the MRD. It is an output of first order filter showing the process of achieving the rheological equilibrium. Its output is difference of effective voltage u_0 and command voltage v with parameter η having unit sec^{-1}. Table 3 provides the parameters obtained using MATLAB (2019b) optimisation toolbox which is very close the experimentally obtained values given in Spencer et al. (1997) and the performance of this model is evaluated through simulation using these parameters in same environment as done in Dyke et al. (1996b) and Spencer et al. (1997) to ensure estimable validation process. The input to simulation process is a standard sinusoidal signal having frequency 2.5 Hz and an amplitude 1.5 cm. Figure 7(a) shows that the force is not zero when the input is zero. This residual force is due to the accumulator section of the MRD as shown in Figure 7(b).

Table 3 Parameters of the generalised MR damper

Parameter	*Value*	*Parameter*	*Value*
c_{0a}	21.0 Nsec/cm	α_a	140 N/cm
c_{0b}	3.50 Nsec/cmV	α_b	695 N/cmV
k_0	46.9 N/cm	γ	363 cm^2
c_{1a}	283 Nsec/cm	β	363 cm^2
c_{1b}	2.95 Nsec/cmV	A	301
k_1	5 N/cm	n	2
z_0	14.3 cm	η	190 sec^{-1}

The results shown in Figures 7(a)–7(c) are very close to the experimentally obtained in the work carried out previously (Spencer et al., 1997). This testing established that this mathematical model can be considered for controller design in the present work.

Figure 7 (a) MRD force due to sinusoid signal (b) Force-displacement (c) Force-velocity (see online version for colours)

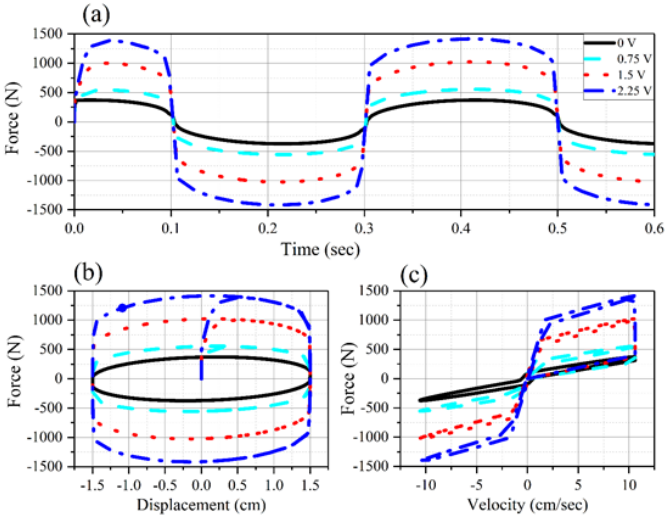

4 Results and discussion

The prototype structure and the MRD model discussed in Sections 3.1 and 3.2 are considered here to validate the results obtained by using the proposed controller. The indicative assembly of the structure equipped with MRD, and the controller is as shown in Figure 8. The results of the proposed controller are carried out under the following conditions.

- using different earthquake time histories
- using an earthquake recorded in different soil conditions
- considering a hypothetical situation where power is lost at the peak of the earthquake.

Moreover, a new parameter of the performance analysis known as cumulative energy is introduced to compute the energy confined in the displacement signal recorded at the top floor. It indicates the damaging capability of the signal. The cumulative energy (W) is mathematically defined in equation (29).

$$W = \int_0^t |z_t|^2 dt \tag{29}$$

4.1 Using different earthquake time histories

Comprehensive performance analysis of the adaptive controller is carried out by comparing the structural responses obtained using the proposed controller and normal

clipped optimal LQG controller on a prototype structure. For proper validation, the value of CWM '**R**' as well as SWM '**Q**' is kept unchanged as in Dyke et al. (1996b). The responses are obtained using different earthquake time-histories. Figures 8(a)–8(c) show the earthquake acceleration time-histories used for this analysis.

Figure 8 (a) El-Centro (b) Chi-Chi (c) Gebze (see online version for colours)

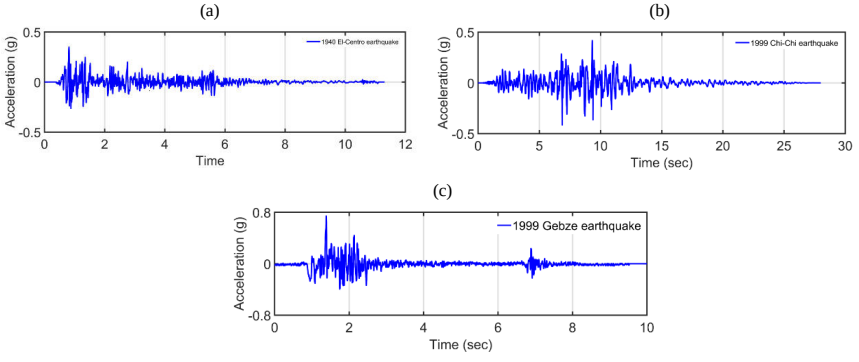

Two popular methodologies (i.e., qualitative and quantitative analysis) are employed to examine the efficacy of the proposed controller. For qualitative analysis, a visual inspection of the time histories of the relative displacements of the third floor of the structure using adaptive LQG (PSO-FFT-modified-LQG) and clipped optimal-LQG (CO-LQG) is performed. Whereas the comparison of the reductions in the peak values of the structural responses for all three floors using a proposed controller and the CO-LQG controller is carried out for quantitative analysis.

Initial 5 sec of time histories of structural responses of the third floor of test structure subjected to El-Centro earthquake is shown in Figure 9. The reason is that the maximum energy is confined in the initial five seconds of the El-Centro earthquake. Figure 9(a) shows the displacement time history of the structure without using any controller (i.e., uncontrolled). Figure 9(b) shows the comparison of displacement time histories of uncontrolled and using the proposed controller as well as the CO-LQG whereas the comparison of the time histories obtained using CO-LQG and PSO-FFT-modified-LQG is demonstrated in Figure 9(c). Figures 9(a)–9(c) indicate that the relative displacement is reduced significantly using the controller. Quantitatively, the proposed controller reduces the uncontrolled relative displacement 5% more than CO-LQG. Further, the changes in the CWM **R** are shown in Figure 9(e). The value of **R** is changed in real time and determined optimally using the PSO algorithm whereas for CO-LQG it remains the same throughout the time. In this way, the control force is used intelligently.

All reductions in the structural responses are achieved using lesser control force as shown in Figure 9(d). The proposed controller utilised 24% lesser force (peak value) to achieve the above-mentioned results as compared with the CO-LQG. Comparison of the energy confined in the signal of the relative displacement of the third floor due to CO-LQG and the proposed controllers is shown in Figure 9(f) which confirms that the displacement signal due to the proposed controller has the lesser energy for destruction as compared with that of CO-LQG.

Figure 9 Structural responses of the third floor using CO-LQG and PSO-FFT-modified-LQG under El-Centro earthquake, (a) displacement response of uncontrolled structure (b) comparison of uncontrolled response with controlled responses (c) comparison of controlled responses (d) comparison of control forces (e) variation of **R** with time (f) comparison of cumulative energies (see online version for colours)

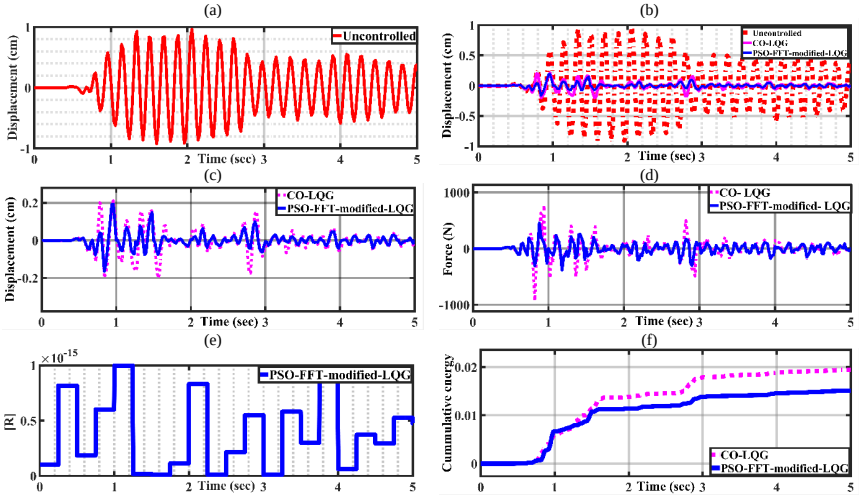

Figure 10 Percentage reduction in the peak values of the responses of the structure subjected to the different time histories using CO-LQG and PSO-FFT-CO-LQG, (a) relative displacement (b) inter-storey drift (c) absolute acceleration (d) control force (see online version for colours)

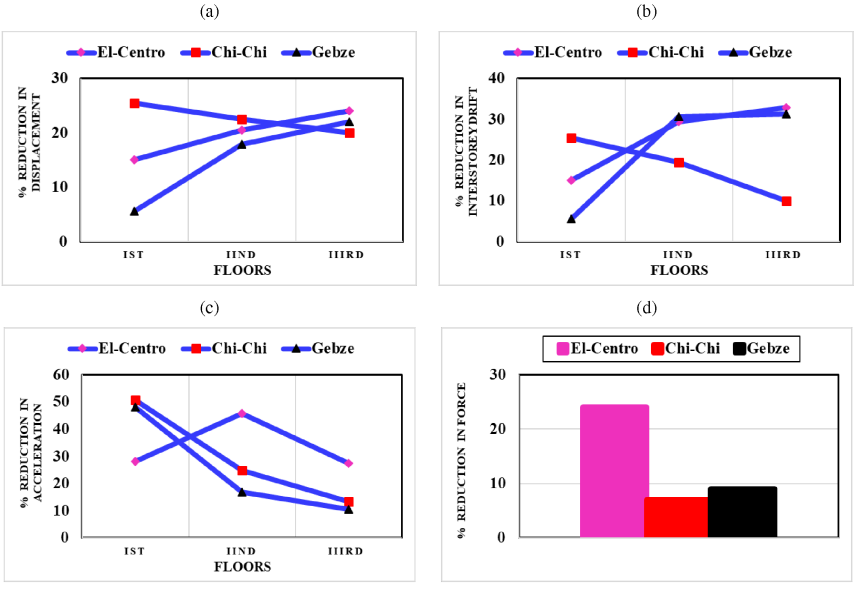

Table 4 Peak structural responses under different seismic signatures

Controller name	*El-Centro earthquake*				*Chi-Chi earthquake*				*Gebze earthquake*			
	Z_t (cm)	$Z_{t_{id}}$ (cm)	Z_a (cm/s^2)	F (N)	Z_t (cm)	$Z_{t_{id}}$ (cm)	Z_a (cm/s^2)	F (N)	Z_t (cm)	$Z_{t_{id}}$ (cm)	Z_a (cm/s^2)	F (N)
Uncontrolled	0.55	0.55	870	0	0.14	0.14	181	0	0.0741	0.0741	126	0
	0.83	0.29	1070		0.22	0.08	268		0.1165	0.0424	150	
	0.97	0.14	1400		0.27	0.05	317		0.1381	0.0216	185	
Passive OFF	0.22	0.22	422	259	0.03	0.03	63	796	0.0177	0.0177	64	475
	0.37	0.15	487		0.04	0.01	83		0.0351	0.0174	67	
	0.47	0.10	721		0.05	0.01	93		0.0497	0.0146	105	
Passive ON	0.08	0.08	284	1,000	0.02	0.02	52	1,535	0.0168	0.0168	56	1,296
	0.20	0.12	498		0.04	0.02	63		0.0343	0.0175	92	
	0.31	0.11	771		0.05	0.01	100		0.0506	0.0163	114	
Quasi bang-bang	0.13	0.13	521	1,005	0.02	0.02	204	1,406	0.0169	0.0169	93	1,145
	0.20	0.08	731		0.03	0.01	73		0.0343	0.0174	101	
	0.30	0.10	727		0.04	0.01	106		0.0503	0.016	120	
CO-LQR	0.12	0.12	733	900	0.03	0.03	38	1,398	0.021	0.021	81	1,080
	0.19	0.07	755		0.05	0.02	63		0.0342	0.013	95	
	0.22	0.03	723		0.06	0.01	101		0.06	0.026	114	
CO-LQG	0.12	0.12	733	900	0.25	0.25	41	1,200	0.022	0.02	86	980
	0.19	0.07	755		0.32	0.07	69		0.035	0.01	90	
	0.22	0.03	723		0.38	0.06	121		0.062	0.03	112	
PSO-FFT-Modified-LQG	0.13	0.13	525	546	0.02	0.02	36	903	0.0200	0.02	59	1,050
	0.22	0.09	417		0.03	0.01	59		0.0300	0.01	68	
	0.30	0.08	530		0.04	0.01	96		0.0500	0.02	105	

Notes: Z_t – relative displacement, $Z_{t_{id}}$ – inter-storey drift, Z_a – absolute acceleration and F – force.

Similar patterns of the results are observed for Chi-Chi and Gebze earthquakes. Figures 10(a)–10(d) demonstrate percentage of reductions in the peak values of the structural responses under different time histories viz. El-Centro, Chi-Chi, and Gebze earthquakes.

From Figure 10(a), the reductions in the peak values of displacement using the proposed controller are by 15%, 21% and 22% for first, second and third floor respectively as compared with the CO-LQG for El-Centro time history. Whereas the same is 26%, 23% and 22% for the Chi-Chi earthquake and 6%, 18%, 22% for Gebze earthquake. For inter-storey drift, the proposed controller achieved reduction by 29% between the first-second floor and 33% between second-third floor as compared with the CO-LQG for El-Centro earthquake, whereas, for the Chi-Chi earthquake, the proposed controller reduces the same by 20% between the first-second and 10% between second-third floor as compared with the CO-LQG. Similarly, for Gebze earthquake, the proposed controller achieves the same by 31% between third-second and second-third floor as compared with CO-LQG as can be seen from Figure 10(b). Alike, the proposed algorithm can reduce the peak values of absolute acceleration by 28%, 46% and 27% for first, second and third floor respectively as compared with the CO-LQG as shown in Figure 10(c) when the structure is subjected to El-Centro earthquake. The percentage reductions in the absolute acceleration for Chi-Chi earthquake are 51%, 25%, 13% whereas for Gebze earthquake, proposed control algorithm achieved reductions in absolute acceleration by 48%, 17%, 10% for first, second and third floor respectively. The proposed controller used 24% lesser force for El-Centro, 7% lesser force for the Chi-Chi earthquake and 9% lesser for Gebze earthquake as compared with the CO-LQG. The cumulative energies are calculated in the displacement time histories of the top floor using proposed controller is observed lesser than the conventional LQG controller for all earthquake time histories. This Indicates the lesser capability of damage in the displacement signal obtained using proposed controller. The peak structural responses under different seismic signatures are presented in Table 4

4.2 Using earthquake recorded in different soil conditions

The soil conditions change the characteristics of ground motions significantly. All the three ground motion characteristics (viz. intensity, frequency and duration) are modified by the soil conditions. The objective of selecting a ground motion recorded in hard, medium and soft soil is to check the effectiveness of the proposed controller. The earthquake is taken from the Kyoshin network (K-NET) recorded in Japan. The soil type is determined according to the federal emergency management agency (FEMA)-356 based on shear wave velocity (v_s) given in Table 5.

Table 5 Classification of soil type

Serial no.	*Shear wave velocity* (v_s)	*Soil type*
1	$>1{,}500$ m/s	Hard soil
2	750 m/s $< v_s <$ 1,500 m/s	Medium soil
3	150 m/s $< v_s <$ 750 m/s	Soft soil

Figure 11 Structural responses of the third floor under the earthquake recorded in hard soil, (a) displacement of uncontrolled structure (b) comparison of uncontrolled and controlled responses (c) comparison of responses due to CO-LQG and proposed controller (d) control forces for the CO-LQG and the proposed controller (e) variation of **R** with time (f) comparison of cumulative energies of the third floor's displacement by applying CO-LQG and proposed controller (see online version for colours)

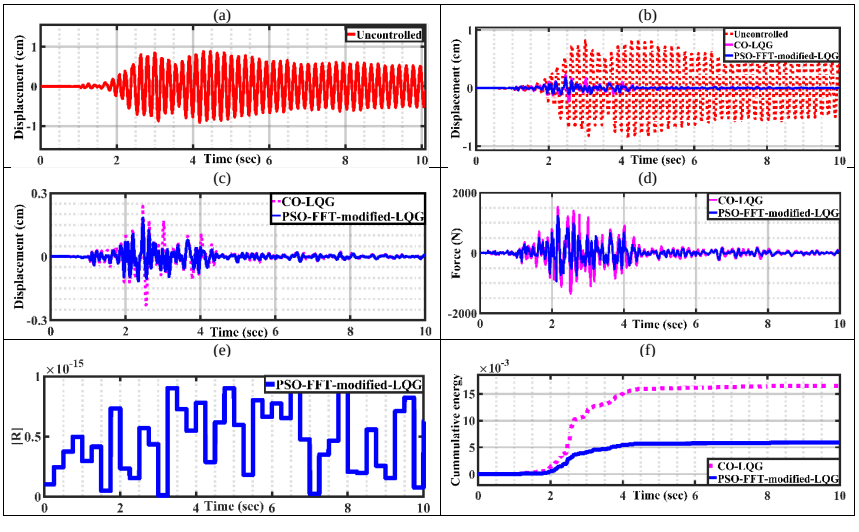

Figure 12 Percentage reduction in the peak values of the responses of the structure subjected to earthquake recorded in the different soils, (a) relative displacement (b) inter-storey drift (c) absolute acceleration (d) control force (see online version for colours)

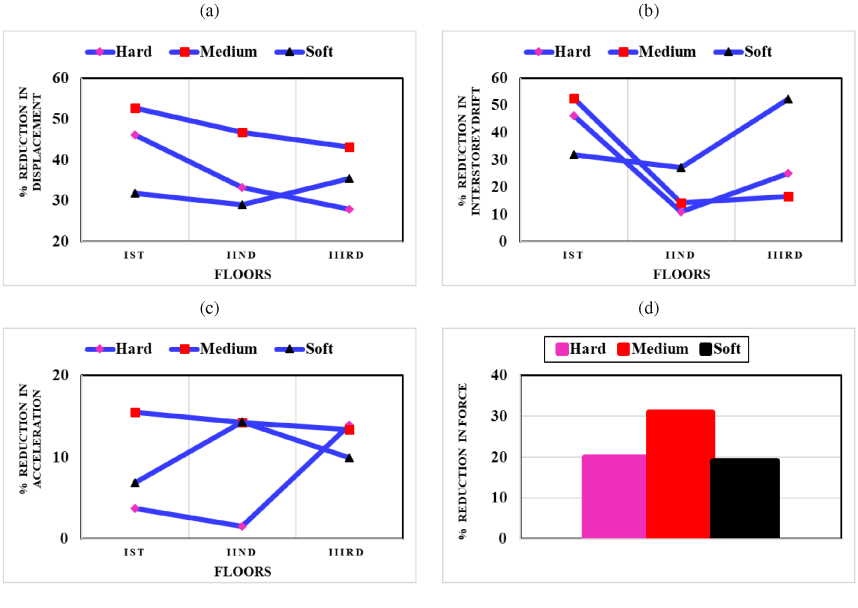

The uncontrolled response of the structure under the hard rock base excitation is shown in Figure 11(a). The visual comparison of uncontrolled and controlled structural response time histories is shown in Figure 11(b). It indicates that the structural control works efficiently for the time history recorded in hard rock soil. The proposed controller surpasses the performance of CO-LQG as demonstrated in Figure 11(c). Variations in the value of **R** are shown in Figure 11(e). According to these variations in control force is determined and applied to the structure. The comparison of cumulative of the energy confined in the signal of displacement of the third floor due to CO-LQG and the proposed controllers is shown in Figure 11(f) which confirms that the displacement signal due to the proposed controller has the lesser energy for destruction as compared with the displacement signal due to the CO-LQG. The similar pattern of the results is observed for earthquake recorded in medium and soft soil conditions as demonstrated in Figures 12(a)–12(d).

It is observed from Figure 12(a), the proposed controller achieved percentage reduction in the relative displacement by 46%, 33% and 28% for first, the second and third floor in peak values as compared with the CO-LQG controller for hard soil earthquake whereas the same are 53%, 47% and 43% for medium soil earthquake and 32%, 29% and 36% for soft soil earthquake. Observing Figure 12(b), for hard soil earthquake, the inter-storey drift is reduced by 12% for the first–second floor and 25% for the second–third floor whereas for medium soil earthquake these are 14%, 17% and 27% and 52% for soft soil earthquake respectively using the proposed controller instead of CO-LQG in the Semi-active control scheme. Similarly, for hard soil, the percentage reduction in absolute accelerations for the first, second and the third floor are 4%, 2% and 14% respectively using the proposed controller whereas for medium soil 15%, 14%, 13% and for soft soil the same are 7%, 14% and 10% respectively as compared with the CO-LQG. Further, the proposed controller attains these reductions in structural responses using 20%, 31% and 19% lesser force than the CO-LQG controller for hard, medium and soft soil respectively as shown in Figure 12(d). Though, there are various factors that affect the behaviour of the structure in different soil. However, the general observation is that the structure located in the relatively soft soil will vibrate more than the structure located in the hard and rocky soil. This is because the soft soil apparently works as an amplifier to the ground motion.

4.3 Effect of the power cut off at the peak of the earthquake

In this objective, a study is carried out for the performance analysis of the proposed controller considering the possibility of power loss during the peak of an earthquake time history. The El-Centro earthquake time history is used for the analysis purpose. The results shown in Figure 13 demonstrate that the semi-active control system converted into the passive off closed loop system and provide a counter force to the structure against the vibrations even if power vanishes. The comparison of the third floor's relative displacement of the uncontrolled structure and the PSO-FFT-modified-LQG controlled structure is shown in Figure 13(a). Power loss is considered at 1 sec of the El-Centro time history since energy in the signal is high at this instant. The PSO-FFT-modified-LQG controller converts into the passive off controller at 1 sec as can be seen in Figure 13(c).

Figure 13 Comparison of the response when power is available for full time and vanishes at the peak (at 1 sec) of earthquake for uncontrolled and proposed controller, (a) comparison of third floor's displacement for uncontrolled and proposed controller (b) comparison of third floor's displacement PSO-FFT-modified-LQG controlled structure (c) comparison of the voltage to the MRD (see online version for colours)

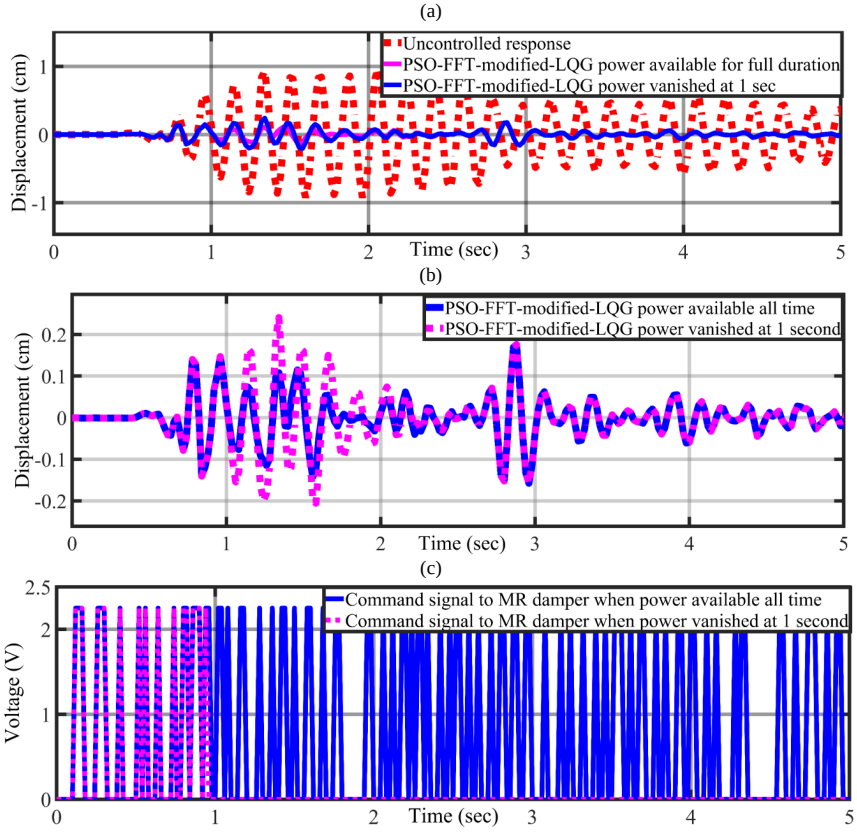

The displacement response of the third floor as shown in Figure 13(a) is lesser than uncontrolled structure. A comparison of third floor's displacement response of structure due to proposed controller before and after 1 sec is shown in Figure 13(b).

5 Conclusions

An algorithm to modify LQG controller is introduced which enables it to utilise the distinctive features of the MRD more efficiently. This modification of the LQG controller is carried out using the fast Fourier transform and the particle swarm optimisation (FFT-PSO) approach. Firstly, the advantage of the advised approach is that the control weighting matrix **R** can be altered during the earthquake to get the optimum response from the proposed controller unlike conventional LQG controller. Additionally, it enhances the performance of the controller by saving the extra energy

for non-resonant bands (i.e., the time interval where no resonance occurs between earthquake and structure). Secondly, the performance of the proposed algorithm has been numerically tested on a three-storey benchmark structure equipped with a MRD, and subjected time histories recorded in near, far fault sites and in different soil conditions. Under these testing conditions, the proposed controller performs superior to the normal LQG controller. For El-Centro earthquake the improvement in the reduction of relative displacement, inter-storey drift and the absolute acceleration is observed 22%, 27% and 33%, respectively. Similarly, for Chi-Chi earthquake the improvements in the structural responses are 22%, 10%, 13% and for Gebze earthquake, 22%, 31%, 10%, respectively. In addition to this, the performance of the proposed controller is also observed better than the conventional LQG controller in different soils viz. Hard, medium and soft soils. Finally, the performance of the modified controller is studied when electric power vanishes at the peak of excitation. The results indicate that the proposed controller works similar to the Passive ON controller in this situation. The lesser cumulative energy in the displacement signal using proposed controller indicates its lesser damage capability as compared to conventional LQG controller. Therefore, based on the results and discussion, the modified LQG controller can be suggested as a good choice for a semi-active control scheme. However, very fast digital signal processors are available for successful implementation of complex algorithms but the use of PSO introduces time delay in the overall system which is a serious issue in seismic conditions. This work may be extended in future to minimise this time delay. Moreover, the experimental verification of the proposed approach is highly recommended for future work.

6 Outcome of this work

This work has the following outcomes

- an approach for modification and tuning of the conventional LQG controller is proposed
- classic PSO and FFT are utilised to tune the weighting matrices in the proposed controller
- a parametric study has been carried out for the evaluation of the proposed controller
- the proposed controller is also evaluated amid the conditions where power is vanished at the peak of the earthquake.

Acknowledgements

The first author is thankful to the leadership at Alliance University, Bengaluru and College of Engineering Roorkee for their support.

References

Abdalla, M., Boulaaras, S. and Akel, M. (2021) 'On Fourier-Bessel matrix transforms and applications', *Mathematical Methods in the Applied Sciences*, Vol. 44, No. 14, pp.11293–11306.

Abderrezek, H., Aissa, A. and Harmas, M.N. (2019) 'Modified pso-based nonlinear controllers applied to a DC-DC converter', *International Journal of Automation and Control*, Vol. 13, No. 1, pp.1–16.

Amezquita-Sanchez, J.P., Dominguez-Gonzalez, A., Sedaghati, R., Romero-Troncoso, R.J. and Osornio-Rios, R.A. (2014) 'Vibration control on smart civil structures: a review', *Mechanics of Advanced Materials and Structures*, Vol. 21, No. 1, pp.23–38.

Amini, F. and Samani, M.Z. (2014) 'A wavelet-based adaptive pole assignment method for structural control', *Computer-Aided Civil and Infrastructure Engineering*, Vol. 29, No. 6, pp.464–477.

Askari, M., Li, J. and Samali, B. (2011) 'Semi-active LQG control of seismically excited nonlinear buildings using optimal Takagi-Sugeno inverse model of MR dampers', *Procedia Engineering*, Vol. 14, pp.2765–2772 [online] https://doi.org/10.1016/j.proeng.2011.07.348.

Barkefors, A., Sternad, M. and Brännmark, L.J. (2014) 'Design and analysis of linear quadratic Gaussian feedforward controllers for active noise control', *IEEE/ACM Transactions on Audio Speech and Language Processing*, Vol. 22, No. 12, pp.1777–1791.

Basu, B. and Nagarajaiah, S. (2008) 'A wavelet-based time-varying adaptive LQR algorithm for structural control', *Engineering Structures*, Vol. 30, No. 9, pp.2470–2477.

Basu, B. and Nagarajaiah, S. (2010) 'Multiscale wavelet-LQR controller for linear time varying systems', *Journal of Engineering Mechanics – ASCE*, Vol. 136, No. 9, pp.1143–1151.

Bhaiya, V., Shrimali, M., Bharti, S. and Datta, T. (2019) 'Modified semiactive control with MR dampers for partially observed systems', *Engineering Structures*, Vol. 191, pp.129–147 [online] https://doi.org/10.1016/j.engstruct.2019.04.063.

Boulaaras, S. (2017) 'Some new properties of asynchronous algorithms of theta scheme combined with finite elements methods for an evolutionary implicit 2-sided obstacle problem', *Mathematical Methods in the Applied Sciences*, Vol. 40, No. 18, pp.7231–7239.

Boulaaras, S. and Doudi, N. (2020) 'Global existence and exponential stability of coupled Lamé system with distributed delay and source term without memory term', *Boundary Value Problems*, Vol. 2020, No. 1, pp.1–21.

Casciati, F., Rodellar, J. and Yildirim, U. (2012) 'Active and semi-active control of structures – theory and applications: a review of recent advances', *Journal of Intelligent Material Systems and Structures*, Vol. 23, No. 11, pp.1181–1195.

Chandrasekar, G., Boulaaras, S.M., Murugaiah, S., Gnanaprakasam, A.J. and Cherif, B.B. (2021) 'Analysis of a predator-prey model with distributed delay', *Journal of Function Spaces*, Vol. 2021, No. 9954409, pp.2314–8896.

Choi, K.M., Cho, S.W., Jung, H.J. and Lee, I.W. (2004) 'Semi-active fuzzy control for seismic response reduction using magnetorheological dampers', *Earthquake Engineering & Structural Dynamics*, Vol. 33, No. 6, pp.723–736.

Choi, S.B., Li, W., Yu, M., Du, H., Fu, J. and Do, P.X. (2016) 'State of the art of control schemes for smart systems featuring magneto-rheological materials', *Smart Materials and Structures*, Vol. 25, No. 4, p.43001.

Collins, E.G. and Selekwa, M.F. (2002) 'A fuzzy logic approach to LQG design with variance constraints', *IEEE Transactions on Control Systems Technology*, Vol. 10, No. 1, pp.32–42.

Dong, X-M., Yu, M., Liao, C-R. and Chen, W-M. (2010) 'Comparative research on semi-active control strategies for magneto-rheological suspension', *Nonlinear Dynamics*, Vol. 59, No. 3, pp.433–453.

Dyke, S., Spencer Jr, B., Quast, P., Sain, M., Kaspari Jr, D. and Soong, T. (1996a) 'Acceleration feedback control of MDOF structures', *Journal of Engineering Mechanics*, Vol. 122, No. 9, pp.907–918.

Dyke, S.J., Spencer Jr., B.F., Sain, M.K. and Carlson, J.D. (1996b) 'Modeling and control of magnetorheological dampers for seismic response reduction', *Smart Materials and Structures*, Vol. 5, No. 5, p.565.

El-Sayed, A.A.E., Boulaaras, S. and Sweilam, N. (2021) 'Numerical solution of the fractional-order logistic equation via the first-kind Dickson polynomials and spectral tau method', *Mathematical Methods in the Applied Sciences* [online] https://doi.org/10.1002/mma.7345.

Fessi, R. and Bouallègue, S. (2019) 'LQG controller design for a quadrotor uav based on particle swarm optimisation', *International Journal of Automation and Control*, Vol. 13, No. 5, pp.569–594.

Garrido, H., Curadelli, O. and Ambrosini, D. (2018) 'On the assumed inherent stability of semi-active control systems', *Engineering Structures*, Vol. 159, pp.286–298 [online] https://doi.org/10.1016/j.engstruct.2018.01.009.

Housner, G.W., Bergman, L.A. and Spencer, B. (1997) 'Structural control: past, present, and future', *Journal of Engineering Mechanics*, Vol. 123, No. 9, pp.897–971.

Hu, J., Wu, H., Zhong, B. and Xiao, R. (2020) 'Swarm intelligence-based optimisation algorithms: an overview and future research issues', *International Journal of Automation and Control*, Vol. 14, Nos. 5–6, pp.656–693.

Ismail, M., Ikhouane, F. and Rodellar, J. (2009) 'The hysteresis Bouc-Wen model, a survey', *Archives of Computational Methods in Engineering*, Vol. 16, No. 2, pp.161–188.

Jansen, L.M. and Dyke, S.J. (2002) 'Semiactive control strategies for MR dampers: comparative study', *Journal of Engineering Mechanics*, Vol. 126, No. 8, pp.795–803.

Kandasamy, R., Cui, F. and Townsend, N. (2016) 'A review of vibration control methods for marine offshore structures', *Ocean Engineering*, Vol. 127, pp.279–297 [online] https://doi.org/10.1016/j.oceaneng.2016.10.001.

Kumar, G., Kumar, A., and Jakka, R.S. (2018) 'An adaptive LQR controller based on pso and maximum predominant frequency approach for semi-active control scheme using MR damper', *Mechanics & Industry*, Vol. 19, No. 1, p.109.

Maiti, R., Sharma, K.D. and Sarkar, G. (2018) 'PSO based parameter estimation and PID controller tuning for 2-DOF nonlinear twin rotor MIMO system', *International Journal of Automation and Control*, Vol. 12, No. 4, pp.582–609.

Miladi, Y., Derbel, N. and Feki, M. (2021) 'Optimal control based on multiple models approach of chaotic switched systems, application to a stepper motor', *International Journal of Automation and Control*, Vol. 15, No. 2, pp.240–258.

Miyamoto, K., She, J., Sato, D. and Yasuo, N. (2018) 'Automatic determination of LQR weighting matrices for active structural control', *Engineering Structures*, Vol. 174, pp.308–321 [online] https://doi.org/10.1016/j.engstruct.2018.07.009.

Panariello, G.F., Betti, R. and Longman, R.W. (1997) 'Optimal structural control via training on ensemble of earthquakes', *Journal of Engineering Mechanics*, Vol. 123, No. 11, pp.1170–1179.

Saaed, T.E., Nikolakopoulos, G., Jonasson, J.E. and Hedlund, H. (2015) 'A state-of-the-art review of structural control systems', *Journal of Vibration and Control*, Vol. 21, No. 5, pp.919–937.

Sari, N.N., Jahanshahi, H., Fakoor, M., Volos, C. and Nikpey, P. (2020) 'Optimal robust control approaches for a geostationary satellite attitude control', *International Journal of Automation and Control*, Vol. 14, No. 3, pp.333–354.

Shafieezadeh, A., Ryan, K. and Chen, Y. (2008) 'Fractional order filter enhanced LQR for seismic protection of civil structures', *Journal of Computational and Nonlinear Dynamics*, Vol. 3, No. 2, pp.21404–21407.

Spencer, B.F., Dyke, S.J., Sain, M.K. and Carlson, J.D. (1997) 'Phenomenological model for magnetorheological dampers', *Journal of Engineering Mechanics*, Vol. 123, No. 3, pp.230–238.

Spencer, B.F. and Nagarajaiah, S. (2003) 'State of the art of structural control', *Journal of Structural Engineering*, Vol. 129, No. 7, pp.845–856.

Symans, M.D. and Constantinou, M.C. (1999) 'Semi-active control systems for seismic protection of structures: a state-of-the-art review', *Engineering Structures*, Vol. 21, No. 6, pp.469–487.

Ullmann, M.R.D., Pimentel, K.F., de Melo, L.A., da Cruz, G. and Vinhal, C. (2017) 'Comparison of PSO variants applied to large scale optimization problems', *2017 IEEE Latin American Conference on Computational Intelligence (LA-CCI)*, pp.1–6.

Wongsathan, C. and Sirima, C. (2008) 'Application of GA to design LQR controller for an inverted pendulum system', *IEEE International Conference on Robotics and Biomimetics, ROBIO*, No. 2, pp.951–954.

Wu, J.L. (2017) 'A simultaneous mixed LQR/H∞ control approach to the design of reliable active suspension controllers', *Asian Journal of Control*, Vol. 19, No. 2, pp.415–427.

Yang, G., Spencer Jr., B.F. and Jung, H.J. (2004) 'Dynamic modeling of large-scale magnetorheological damper systems for civil engineering applications', *Journal of Engineering Mechanics*, Vol. 130, No. 9, pp.1107–1114.